Redistribution of phosphorus during Ni 0.9 Pt 0.1 -based silicide formation on phosphorus implanted Si substrates

M. Lemang, Ph. Rodriguez, F. Nemouchi, M. Juhel, M. Grégoire, Dominique Mangelinck

Redistribution of phosphorus during $Ni_{0.9}Pt_{0.1}$-based silicide formation on phosphorus implanted Si substrates

M. Lemang,[1,2,3,a] Ph. Rodriguez,[2] F. Nemouchi,[2] M. Juhel,[1] M. Grégoire,[1] and D. Mangelinck[3]
[1] *STMicroelectronics, 850 rue Jean Monnet, BP 16, 38926 Crolles, France*
[2] *Univ. Grenoble Alpes, F-38000 Grenoble, France*
CEA, LETI, MINATEC Campus, F-38054 Grenoble, France.
[3] *CNRS, Aix Marseille Université, IM2NP (UMR 7334) Faculté de Saint-Jérôme, F-13397 Marseille Cedex, France*

(Dated: 1 February 2018)

The phosphorus diffusion and its distribution during the solid-state reactions between $Ni_{0.9}Pt_{0.1}$ and implanted Si substrates are studied. The silicidation is achieved through a first rapid thermal annealing followed by a selective etching and a direct surface annealing. The redistribution of phosphorus in the silicides layers is investigated after the first annealing for different temperatures and after the second annealing. Phosphorus concentration profiles obtained thanks to ToF-SIMS and atom probe tomography characterizations for partial and total reaction of the deposited 7 nm thick $Ni_{0.9}Pt_{0.1}$ film are presented. Phosphorus segregation is observed at the $Ni_{0.9}Pt_{0.1}$ surface and at Ni_2Si interfaces during the Ni_2Si formation and at the NiSi surface and the NiSi / Si interface after NiSi formation. The phosphorus is evidenced in low concentrations in the Ni_2Si and NiSi layers. Once NiSi is formed, a bump in the phosphorus concentration is highlighted in the NiSi layer before the NiSi / Si interface. Based on these profiles, a model for the phosphorus redistribution is proposed to match this bump to the former Ni_2Si / Si interface. It aims also to bind the phosphorus segregation and its low concentration in the different silicides to a low solubility of the phosphorus in Ni_2Si and in NiSi and a fast diffusion of phosphorus at their grain boundaries. This model is also substantiated by a simulation using a finite difference method in one dimension.

PACS numbers: 61.72.uf, 68.35.bg, 68.35.bd, 81.05.Je, 81.70.Jb, 82.80.Ms, 85.40.Ls, 85.40.Ry
Keywords: silicide, phosphorus, dopant, NiSi, ToF-SIMS, Atom Probe Tomography

I. INTRODUCTION

In microelectronic field and especially for the FDSOI (Fully depleted Silicon On Insulator) CMOS technologies, a major concern is to form a contact between the active regions and the interconnections of a device[1]. To achieve this the salicide process is used and allows obtaining a silicide intermetallic compound by the solid-state reaction between a metal or an alloy and a doped semiconductor without lithography alignment. For many years, the silicides used were $TiSi_2$ and $CoSi_2$. However, started from the sub 90 nm node, NiSi has replaced them because of many of its advantages such as no narrow line effect and a lower Si consumption[1,2]. Nonetheless the Ni-Si system owns its own drawbacks such as the highly-resistive $NiSi_2$ phase formation[2] and NiSi agglomeration[3]. Nowadays, depending on the most advanced CMOS technology, Ti-silicide (FinFet) or NiPt-silicide (FDSOI) are formed on the active region in order to further decrease the contribution of the interface resistance. The present study was conducted in the frame of advanced NiPt thin silicide formed on n-doped silicon substrates with phosphorus.

Ni-based silicidation with thin films usually follows a sequential growth[4]. The first phase to form is a Ni_2Si silicide of which the crystallographic structure depends on the experimental conditions[5,6]. A transient phase may appear in some cases[7]. Then, Ni_2Si reacts with Si to form NiSi and finally NiSi reacts with Si to form $NiSi_2$[4]. The addition of Pt was introduced in order to delay the unwanted $NiSi_2$ formation[8] and to shift NiSi agglomeration temperature[3].

Additionally, in devices and in particular on FD-SOI, thin NiPt-silicides grow on heavily doped Si. Dopants can modify the silicide formation or the film properties because it requires thermal budgets that are high enough to induce a redistribution of dopants. The behavior of dopants presents a huge interest regarding the fact that it has an impact on the junction performances and yield issues. Indeed, the dopant concentration in the semiconductor is mainly responsible for Schottky barrier height and thus for the ohmic or Schottky behavior of a contact[9,10]. To this extent, it is mandatory to assess and understand the dopant diffusion and distribution during the silicide formation.

Most of the studies on dopant and silicide formation deal with samples doped by ionic implantation of arsenic and boron[9–15]. These studies report different behaviors such as snowplowing, uniform redistribution in the silicide, or pile-up at the silicide surface and at silicide / silicon interface[9,16]. Dopants redistribution studies have shown that B accumulated at NiSi surface and at NiSi / Si interface, and that B-rich clusters were formed in the NiSi part closer to the NiSi / Si interface[12,14,15]. Arsenic has been reported to pile-up at the interfaces dur-

[a] Corresponding author; E-mail: mathilde.lemang@st.com

ing the Ni_2Si formation[11] and at the NiSi interfaces[17]. Fewer studies have been carried out on phosphorus redistribution. During the PtSi formation, implanted phosphorus atoms pile up near the PtSi / Si interface[18], while in a NiSi system no pile-up is observed at any of the NiSi interfaces[19].

In the present work, the formation of up-to-date silicide by the reaction of Pt-enriched Ni with phosphorus doped Si is examined. The effects of a two steps annealing on the redistribution of implanted phosphorus are investigated. Moreover, this study aims also to deeper explain the physical mechanisms that led to such dopant redistribution by using experimental characterization, and modeling of the phosphorus diffusion during the silicidation.

II. EXPERIMENTAL PROCEDURE

A first set of samples is carried out on intrinsic silicon. Before metal deposition, Si wafers were cleaned by HF 0.5 % solution and by in situ dry NF_3 / NH_3 based chemical etch and anneal (Siconi^{TM} process). A 7 nm thick $Ni_{0.9}Pt_{0.1}$ film and a 7 nm thick TiN capping layer were deposited by magnetron sputtering within the same equipment to avoid air breaks. The samples were silicided at different rapid thermal annealing (RTA1) temperatures for 30 s. Afterwards, the unreacted $Ni_{0.9}Pt_{0.1}$ and the TiN capping layer were removed by wet selective etching (SE) in H_2O_2 / H_2SO_4 / H_2O (SPM) and NH_4OH / H_2O_2 / H_2O (SC1)chemical reactions. The sheet resistance is measured on these samples.

Another set of samples was prepared on doped Si blanket wafers. The phosphorus was implanted with a dose of $2.7x10^{15}$ at/cm^2 and an energy of 2 keV in monocrystalline silicon. A spike annealing at 1050 ℃ was performed to activate the dopants and to recover the damaged Si. The final maximum concentration in the samples is $6x10^{21}$ at/cm^3. Afterward, $Ni_{0.9}Pt_{0.1}$ silicidation process was applied as described in Fig. 1. After the native oxide removal by in situ Siconi^{TM}, a 7 nm thick $Ni_{0.9}Pt_{0.1}$ film and a TiN capping layer were deposited by magnetron sputtering on phosphorous doped Si blanket wafers within the same equipment. After the metal deposition, a two annealing steps silicidation was achieved with a first 20 s rapid thermal annealing (RTA1) at temperatures of 230 and 270 ℃. A direct surface annealing (DSA2) at 815 ℃ was then processed on a part of the samples as second annealing to form NiSi. Between the annealing steps, the unreacted $Ni_{0.9}Pt_{0.1}$ and the TiN capping layer were removed by the same wet selective etching (SE) as described formerly. After NiSi formation, a technical protective layer of $Ni_{0.85}Pt_{0.15}$ is deposited to cap and prevent silicide surface from contamination, oxidation, or chemical/mechanical damages during Atom Probe Tomography (APT) sample preparation.

Depth profiles were performed thanks to time of flight secondary ion mass spectrometry (ToF-SIMS) using a 500 eV Cs^+ beam. The concentration of the different elements were analyzed by APT. The APT samples were machined by Ga^+ beam to shape tips using the annular milling method. The measurements were carried out thanks to Imago Leap 3000 HR microscope at 50 K, using femtosecond laser pulses with an energy of 0.5 nJ. For the 3D reconstruction of the tip, peaks of given mass to charge state ratio are assigned to elements. In the samples, two masses related to phosphorus are detected: $^{31}P^{2+}$ and $^{31}P^+$. However, the $^{31}P^+$ peak has the same position as the $^{62}Ni^{2+}$ one. So in the silicide this peak overlaps with the nickel one because nickel is a majority element in NiSi in comparison to phosphorus. However, in the Si substrate the $^{31}P^+$ peak is only related to phosphorus.

Modeling of P redistribution was accomplished using a finite difference method in one dimension similar to the one developped by Blum[12].

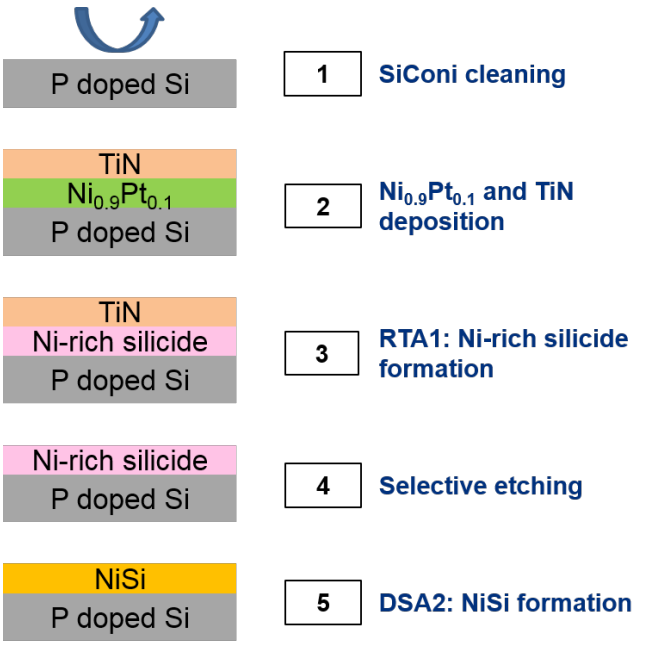

FIG. 1. Description of two annealing steps silicidation process.

III. RESULTS

A. Silicidation with intrinsic silicon

Figure 2 represents the sheet resistance (Rs) at different stages for various RTA1 temperatures after the selective etch process. From 220 ℃ to 280 ℃, the sheet resistance decreases indicating the formation of a Ni-rich silicide. The sheet resistance decrease from 270 to 130 Ω/□ is linked to the increase of the thickness of the Ni-rich silicide. The total consumption of $Ni_{0.9}Pt_{0.1}$ seems to occur between 240 and 260 ℃ where the sheet resistance reaches a plateau at 135 Ω/□. Beyond 280 ℃, the Ni-

rich silicide starts its conversion into mono-silicide leading to a decrease of the sheet resistance as NiSi is the less resistive phase. At 300 ℃, the sheet resistance reaches the lowest Rs of 20 Ω/□ indicating that NiSi is totally formed. Finally at 800 ℃, the sheet resistance skyrockets to 300 Ω/□ as NiSi agglomerates. To conclude, a Ni-rich silicide forms first and when the metal consumption is total (280 ℃ for 30 s), the film is transformed in NiSi. Following these observations and in order to examine the phosphorus redistribution after the RTA1 for a partial reaction and a total reaction, the temperatures of 230 and 270 ℃ were chosen for the following of the study.

Before looking at the dopant redistribution after silicidation, a knowledge of the Ni-rich silicide phase formed after the RTA1 is necessary. A previous study has shown that for a 11 nm of $Ni_{0.9}Pt_{0.1}$, the θ-Ni_2Si phase is formed preferentially to δ-Ni_2Si[5]. Similar in situ - X-Ray Diffraction (XRD) experiments than the ones in Panciera et al. study[5] have been performed on unreacted samples and give the same phase sequence (same peaks, same temperature). Hence, the Ni-rich silicide in presence after a RTA1 from 180 to 280 ℃ should be the θ-Ni_2Si phase.

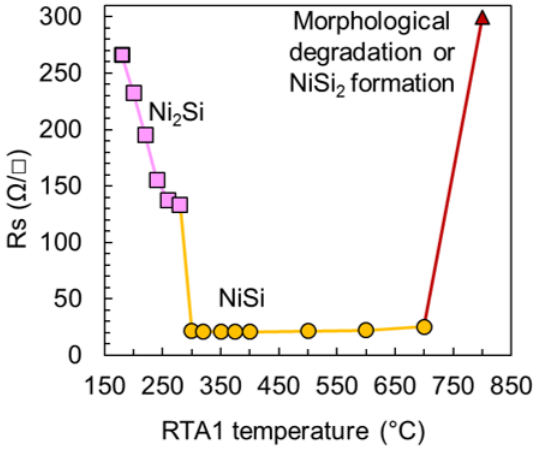

FIG. 2. Rs measurement of silicide after rapid thermal annealing (RTA1) at different temperatures and after the selective etching process.

B. Dopant distribution

1. Phosphorus redistribution after the first Rapid Thermal Annealing (RTA1)

The nickel and phosphorus concentration profiles measured by ToF-SIMS after RTA1 at three different temperatures are respectively presented in Fig. 3a and Fig. 3b. As there are several phases present in one sample (TiN, metal, silicides, Si) and because of the strong matrix effect in SIMS, the raw SIMS data (counts versus sputtering time) were not converted to concentration versus depth.

For RTA1 at 230 ℃ (Fig. 3a), the nickel intensity signal remains low until the erosion time reaches around 200 s which corresponds to the TiN capping layer. From 200 s, the Ni signal increases to reach a maximum and then decreases until a local minimum after 250 s. This corresponds to the $Ni_{0.9}Pt_{0.1}$ layer that has not totally reacted. Afterwards, from 250 to 325 s the Ni intensity signal increases and indicates that Ni_2Si is reached. Then, started from 325 s the Si layer is reached as the intensity of nickel falls.

Regarding the RTA1 temperature of 270 ℃, the unreacted $Ni_{0.9}Pt_{0.1}$ layer is not present. As a consequence, after the TiN layer, from 250 s to 350 s, the increase of Ni intensity signal attests that Ni_2Si is attained. Finally, the Si layer is reached.

Figure 3b represents the phosphorus profiles after the different annealings. First and foremost, the distribution of P in the different layers is not uniform. For the RTA1 at 230 ℃, there is a peak of phosphorus concentration at the $Ni_{0.9}Pt_{0.1}$ surface and at $Ni_{0.9}Pt_{0.1}$ / Ni_2Si and Ni_2Si / Si interfaces. Meanwhile for the RTA1 at 270 ℃, there are two phosphorus peaks, one at Ni_2Si surface and the other at Ni_2Si / Si interface. Moreover, the ToF-SIMS experiments highlight that there is a low concentration of P in the Ni_2Si layer for all RTA1 temperatures.

2. Phosphorus redistribution after the Direct Surface Annealing (DSA2)

The nickel and phosphorus concentration profiles measured by ToF-SIMS after various RTA1 and DSA2 for phosphorus implanted samples are presented in Fig. 4. The nickel and the phosphorus profiles can be divided in different regions. In Fig. 4a, the nickel intensity signal is constant around 80 s until 200 s: this represents the capping layer of $Ni_{0.85}Pt_{0.15}$. Started from 200 s is the second region where the Ni intensity drops. It corresponds to NiSi. The position of the silicide / silicon interface varies depending on the thermal budget applied during RTA1. NiSi is thinner for the RTA1 at 230 ℃ than for the one at 270 ℃. Indeed, the silicon layer is reached at 450 s for RTA1 at 230 ℃, and 550 s for RTA1 at 270 ℃ as the intensity of nickel falls.

Concerning the phosphorus distribution on Fig. 4b, its concentration is higher at the surface of NiSi (t = 200 s) than through the silicide. Actually in NiSi, the profile is nearly flat, with a low amount of phosphorus. The phosphorus concentration increases when the silicide / Si interface is reached at 450 s for RTA1 at 230 ℃, and 550 s for RTA1 at 270 ℃.

Before the silicide / silicon interface, the profile with the RTA1 at 230 ℃ exhibits a bump at t = 400 s. This bump is pointed out with an arrow on Fig. 4b. On the profile for the RTA1 at 270 ℃, this bump is less exacerbated (t = 450 s).

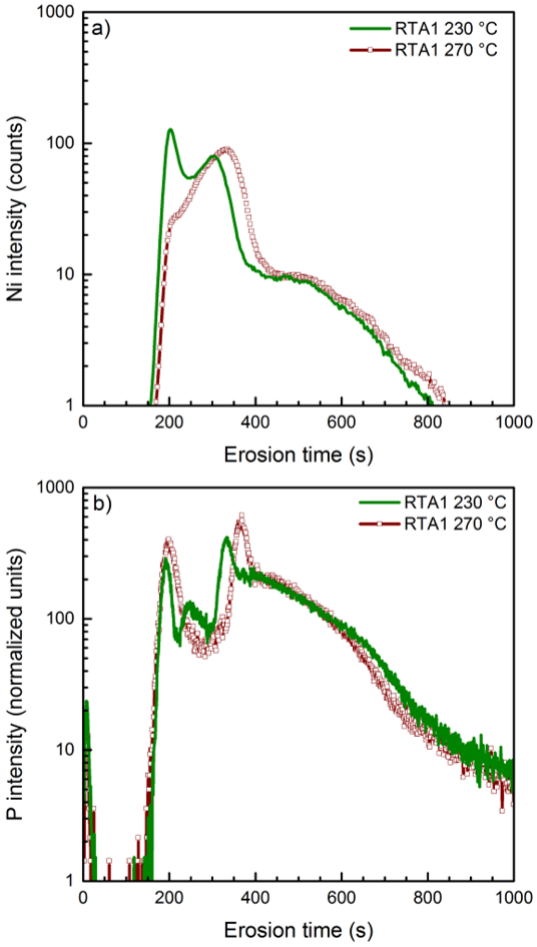

FIG. 3. a) Ni and b) P concentration profiles measured with ToF-SIMS after silicidation at 230 and 270 ℃ for 20 s in P implanted samples.

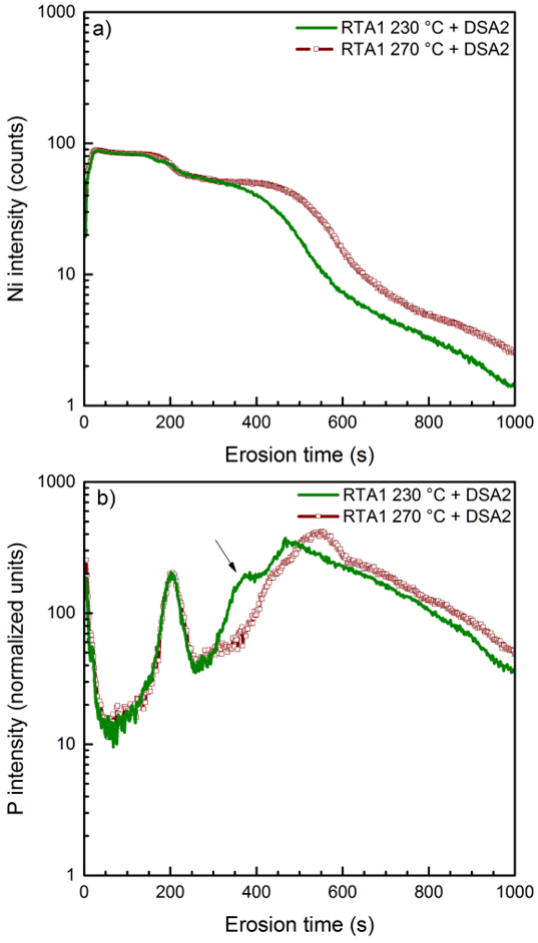

FIG. 4. a) Ni and b) P concentration profiles measured with ToF-SIMS after silicidation at 230 and 270 ℃ for 20 s in P implanted samples followed by a DSA2 at 815 ℃.

Figure 5 represents 1D composition profiles in APT reconstructed volumes of samples silicided after RTA1 at 230 ℃ (Fig. 5a) and at 270 ℃ (Fig. 5b) followed by DSA2. In order to quantify the phosphorus redistribution, 1D composition profiles were determined using cylindrical volumes shown in the inset in Fig. 5a and Fig. 5b. In the silicide, the phosphorus concentrations are given with an error of 12%, the ratio between the background noise and the $^{31}P^{2+}$ mass to charge state ratio peak.

The three different regions previously highlighted are anew noticeable in Fig. 5a and Fig. 5b: the capping, the silicide and the silicon. For the RTA1 at 230 ℃ with DSA2 (Fig. 5a) the NiSi thickness was measured at 12 nm whereas for the RTA1 at 270 ℃ with DSA2 (Fig. 5a) NiSi was 16 nm thick.

Focusing on Ni and Si profiles on Fig. 5a and Fig. 5b, there is a variation of concentration linked to the NiSi surface roughness at the $Ni_{0.85}Pt_{0.15}$ / NiSi interface. In both figures, the phosphorus has a lower concentration in the silicide layer than at its surface and interface for an average concentration of 0.3 % against 1 %. The high concentration of P at the silicide interfaces is also visible in the insets on the Fig. 5.

Besides, for the phosphorus profile at 230 ℃ with DSA2 (Fig. 5a), the bump that was observed at the silicide / silicon interface in Fig. 4b is also visible. Once again, this bump is less discernible on Fig. 5b for the phosphorus profile at of 270 ℃ with DSA2.

IV. THE PHOSPHORUS REDISTRIBUTION DURING THE SILICIDATION

A. Discussion

After the RTA1 at 230 ℃, there is still a layer of $Ni_{0.9}Pt_{0.1}$ (Fig. 3a). The metal has not fully reacted during the RTA1 process and the reaction of formation of Ni_2Si is partial. On the contrary, after the RTA1 at 270 ℃, $Ni_{0.9}Pt_{0.1}$ is fully consumed in order to form the Ni_2Si. A direct consequence is that after the DSA2, the NiSi layer is thicker for RTA1 at 270 ℃ (Fig. 5b), and

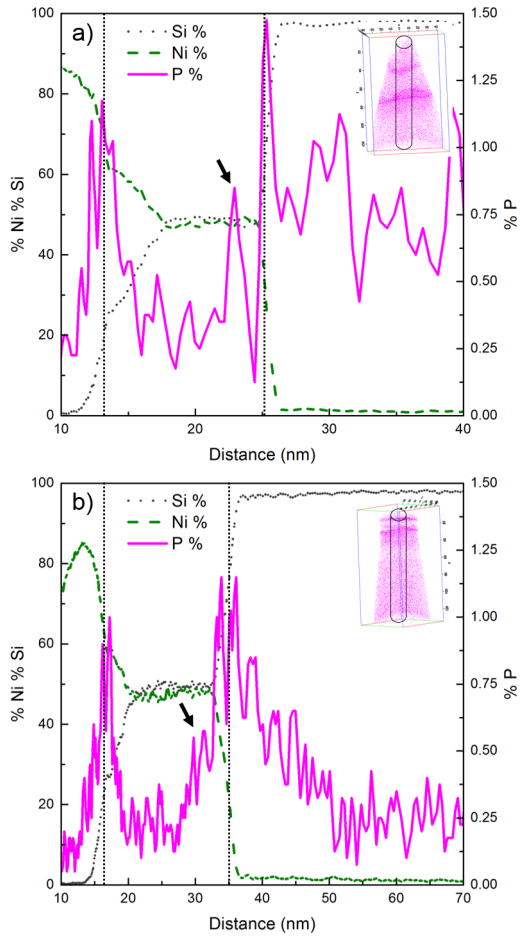

FIG. 5. Ni, Si and P ATP profiles in a sample capped with $Ni_{0.85}Pt_{0.15}$ after a deposition of 7 nm of $Ni_{0.9}Pt_{0.1}$ annealed at a) 230 ℃ and b) 270 ℃ RTA1 followed by a DSA2 at 815 ℃. The phosphorus concentrations have been plotted with the mass to charge ratio of $^{31}P^{2+}$.

that the position of the silicide / silicon interface varies depending on the thermal budget applied during RTA1 on the Fig. 4b. Hence, the quantity of silicon and incorporated phosphorus consumed during the solid-state reaction is higher as the temperature increases.

The phosphorus is observed in low concentration in Ni_2Si probably due to its low solubility in this phase. During the silicidation, the phosphorus redistributes and segregates at $Ni_{0.9}Pt_{0.1}$ surface, at $Ni_{0.9}Pt_{0.1}$ / Ni_2Si and Ni_2Si / Si interfaces (Fig. 3b). For the RTA1 at 270 ℃, as the reaction is total, the phosphorus accumulates at Ni_2Si surface and at Ni_2Si / Si interface. After the DSA2, the phosphorus segregates at the NiSi interfaces and is still in low concentration in the silicide.

The bump shape of the phosphorus profile plotted on Fig. 4b has previously been observed for implanted boron after the Ni silicidation by Blum et al.[12]. It was found to match to the original position of δ-Ni_2Si / Si interface, where the nucleation of NiSi takes place. In this study, this bump would be matched to the θ-Ni_2Si / Si interface as described in Fig. 6. Indeed, it has been suggested that in the present system the first phase that forms would be θ-Ni_2Si.

Figure 6a focuses on this Ni_2Si / Si interface after the SE process. During the DSA2, the growth of NiSi occurs at its both interfaces (Fig. 6b). Indeed at the Ni_2Si / Si interface, Ni_2Si transforms into NiSi while Ni is released. The Ni diffuses towards the NiSi / Si interface and reacts there with Si to obtain NiSi (Fig. 6c). As shown on Fig. 4b, the concentration of phosphorus is lower on NiSi side of the bump (from 200 s to 400 s for RTA1 at 230 ℃) and increases when it comes to the NiSi / Si interface (from 400 s to 450 s for RTA1 at 230 ℃). Finally, the low concentration of P in the silicide and the segregation at its surfaces could be explained by a low solubility of P in the Ni_2Si and a fast diffusion of P along its grain boundaries.

Indeed, during the growth of Ni_2Si, a part of the phosphorus would diffuse preferentially along the grain boundaries to segregate at the surface while the other part accumulates at Ni_2Si / Si. Since the phosphorus solubility is supposed to be low in the NiPt silicides, a low amount of phosphorus should diffuse into the silicide matrix. As a consequence, the amount of phosphorus measured by ToF-SIMS in Ni_2Si represents the phosphorus located in the grain boundaries. After RTA1 and whatever the temperature, the phosphorus amount observed in the silicide comes from the grain boundary density. The same behavior is expected in NiSi with the relative grain boundary density after a SE process and the DSA2.

B. Modeling of phosphorus redistribution

Based on this proposed redistribution scheme, the phosphorus redistribution was modeled using a finite difference method in one dimension as described by Blum[12]. However, the model used in this study takes into account the selective etching process step. The values of the several parameters that were taken into account are presented in Table I.

Besides, the hypothesis was made that the phosphorus diffusion occurs at Ni-based silicide grain boundaries. This results in the following relationship between the different phosphorus diffusion coefficients in the different layers in presence:

$$D^{P}_{Si} \sim D^{P}_{Ni_2Si} \ll D^{P}_{NiSi} \ll D^{P}_{Ni}.$$

Phosphorus redistribution modeling after a partial consumption of $Ni_{0.9}Pt_{0.1}$, a partial formation of NiSi and a complete formation of NiSi are respectively presented in the Fig. 7a, Fig. 7b, and Fig. 7c. The thickness of $Ni_{0.9}Pt_{0.1}$ that reacts at 230 ℃ was chosen to fit the NiSi thicknesses measured by APT. After a reaction equivalent to the RTA1 at 230 ℃ (Fig. 6a), the simulation is consistent with ToF-SIMS profiles presented on Fig. 3b. The phosphorus segregates at $Ni_{0.9}Pt_{0.1}$ surface and at $Ni_{0.9}Pt_{0.1}$ / Ni_2Si and Ni_2Si / Si interfaces.

TABLE I. Segregation, partition and diffusion parameters used for the simulation of P redistribution during Ni silicides formation.

Phase	Surface Segregation	Bulk Partition	Diffusion	Interface	Interfacial segregation
Ni	1	0.02	High	Ni / Ni_2Si	0.1
Ni_2Si	0.1	0.02	High	Ni_2Si / Si	1
NiSi	1	0.02	Medium	Ni_2Si / NiSi	1
Si	-	1	Low	NiSi / Si	0.2

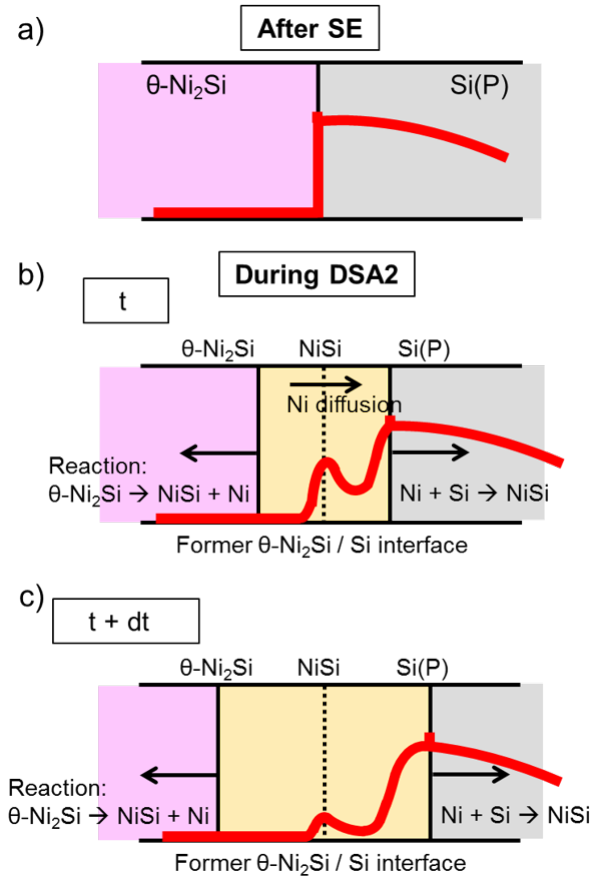

FIG. 6. Phosphorus redistribution pattern proposal after a) selective etching process, b) during DSA2 at time t and c) during DSA2 at time t+dt.

After a RTA1 at 230 ℃ followed by SE and DSA2 (Fig. 7b), NiSi is 10.6 nm thick which is consistent with the APT observations (Fig. 5a). This corresponds to a consumption of 4.5 nm of the deposited $Ni_{0.9}Pt_{0.1}$ layer. After a RTA1 at 270 ℃ followed by SE and DSA2 (Fig. 7b), the thickness of the NiSi layer is 16 nm. This corresponds to a total consumption of the $Ni_{0.9}Pt_{0.1}$ layer. After modeling of RTA1 followed by SE and DSA2, the phosphorus segregates at the interfaces of NiSi as observed in the Fig. 5 and 4b.

Furthermore, the bump before the NiSi / Si interface is less exacerbated for the modeling of the total formation of NiSi as on the previous ToF-SIMS observations (Fig. 4). Therefore, the redistribution model that is proposed and the hypothesis concerning the low solubility of P in the Ni_2Si and a fast diffusion of P at its grain boundaries seems to be valid.

Finally, the low concentration of P in the silicide and the segregation at its surfaces could be explained by a low solubility of P in the Ni_2Si and a fast diffusion of P at its grain boundaries.

V. CONCLUSION

The present work highlighted the diffusion and the distribution of dopants during the silicide formation for a $Ni_{0.9}Pt_{0.1}$ / Si system. A closer look was taken at the effects of a two steps annealing on the redistribution of implanted phosphorus.

When forming the Ni_2Si with a RTA1, it was shown that the phosphorus segregates at the $Ni_{0.9}Pt_{0.1}$ surface and the Ni_2Si interfaces. Moreover, the phosphorus accumulates at the silicide interfaces after the formation of NiSi. Besides, ToF-SIMS and Atom Probe Tomography phosphorus concentration profiles exhibited a bump in NiSi layer before the NiSi / Si interface that would be matched to the former Ni_2Si / Si interface. Finally, a model with a low solubility of P inside the Ni_2Si and a fast diffusion of P at its grain boundaries was proposed to explain the low concentration of P in the silicide and the segregation at its surfaces.

To support this redistribution model, a simulation of the phosphorus redistribution through the different annealing steps was carried out. It is in accordance with the hypothesis of a low solubility of P in the Ni_2Si and a fast diffusion of P at its grain boundaries.

It was shown in the present study that the phosphorus distribution can be influenced by the silicide formation of both Ni_2Si and NiSi phases owing to the phosphorus solubility in the silicides aforementioned, and a controlled grain boundaries density where the dopant diffuses.

ACKNOWLEDGMENTS

This research was supported by the French National Research Agency (ANR) under the “Investissements d’avenir” programs: ANR-10-EQPX-0030 (FDSOI 11), Nano2017 project and by STMicroelectronics-LETI alliance program. The authors would like to thank,

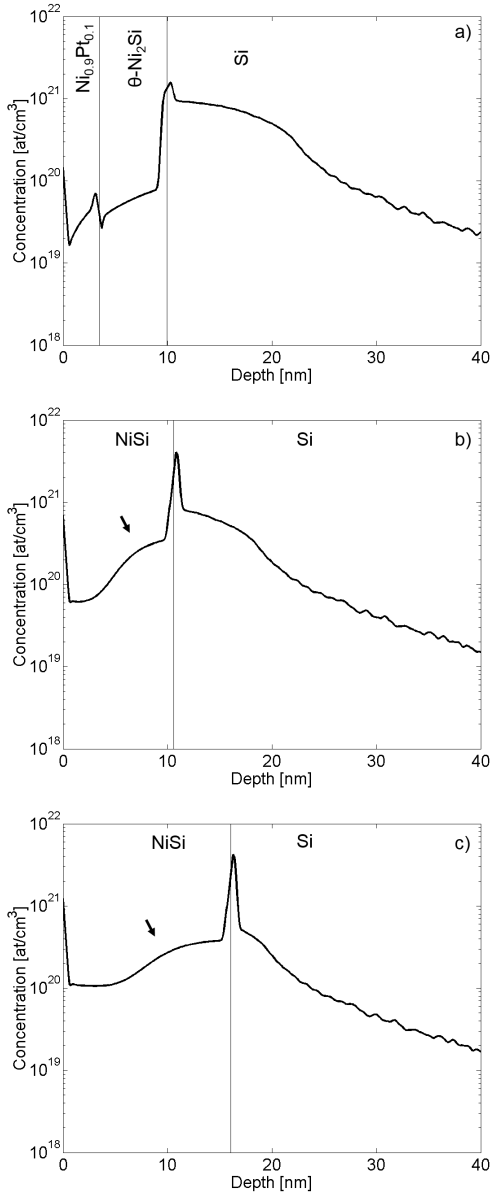

FIG. 7. Phosphorus redistribution modeling after a) RTA1 at 230 ℃ after b) partial formation of NiSi (i.e.) RTA1 at 230 ℃ followed by SE and DSA2, and c) total formation of NiSi (i.e.) RTA1 at 270 ℃ followed by SE and DSA2.

R. Beneyton for rapid thermal annealings and M. Descoins for Atom Probe Tomography characterization.

REFERENCES

[1]H. Iwai, T. Ohguro, and S. Ohmi, Microelectron. Eng. **60**, 157 (2002).
[2]C. Lavoie, F. M. d'Heurle, C. Detavernier, and C. Cabral Jr., Microelectron. Eng. **70**, 144 (2003).
[3]C. Lavoie, C. Detavernier, C. Cabral Jr., F. M. d'Heurle, A. J. Kellock, J. Jordan-Sweet, and J. M. E. Harper, Microelectron. Eng. **83**, 2042 (2006).
[4]P. Gas and F. M. d Heurle, Appl. Surf. Sci. **73**, 153 (1993).
[5]F. Panciera, D. Mangelinck, K. Hoummada, M. Texier, M. Bertoglio, A. De Luca, M. Grégoire, and M. Juhel, Scr. Mater. **78/79**, 9 (2014).
[6]K. De Keyser, C. Van Bockstael, R. L. Van Meirhaeghe, C. Detavernier, E. Verleysen, H. Bender, W. Vandervorst, J. Jordan-Sweet, and C. Lavoie, Appl. Phys. Lett. **96**, 175503 (2010).
[7]S. Gaudet, C. Coia, P. Desjardins, and C. Lavoie, J. Appl. Phys. **107**, 093515 (2010).
[8]D. Mangelinck, J. Y. Dai, J. S. Pan, and S. K. Lahiri, Appl. Phys. Lett. **75**, 1736 (1999).
[9]S. P. Murarka and D. S. Williams, J. Vac. Sci. Tech. B. **5**, 1674 (1987).
[10]K. Hoummada, D. Mangelinck, C. Perrin, V. Carron, and P. Holliger, J. Appl. Phys. **104**, 024313 (2008).
[11]M. A. Pawlak, T. Janssens, A. Lauwers, A. Vantomme, W. Vandervorst, K. Maex, and J. A. Kittl, Appl. Phys. Lett. **87**, 181910 (2005).
[12]I. Blum, A. Portavoce, L. Chow, K. Hoummada, and D. Mangelinck, Defect and Diffusion Forum **323-325**, 415 (2012).
[13]Y.-L. Jiang, A. Agarwal, G.-P. Ru, X.-P. Qu, and B.-Z. Li, 4th Internat. Workshop on Junction Technology , 139 (2004).
[14]A. Portavoce, I. Blum, D. Mangelinck, K. Hoummada, L. Chow, V. Carron, and J. L. Lábár, Scr. Mater. **64**, 828 (2011).
[15]O. Cojocaru-Mirédin, C. Perrin-Pellegrino, D. Mangelinck, and D. Blavette, Microelectron. Eng. **87**, 271 (2010).
[16]M. Wittmer and T. E. Seidel, J. Appl. Phys. **49**, 5827 (1978).
[17]K. Hoummada, G. Tellouche, I. Blum, A. Portavoce, and D. Mangelinck, Scr. Mater. **67**, 169 (2012).
[18]A. Kikuchi and S. Sugaki, J. Appl. Phys. **53**, 3690 (1982).
[19]H. Takai and K. N. Tu, Phys Rev B **38**, 8121 (1988).